Original Article

Measurement of aortofemoral volume wave velocity during the routine 12-channel ECG: relation to age, physiological hemoglobin A1c, triglycerides and SBP in healthy individuals

Falko Skrabal[a], Thomas Weber[b], Katharina Skrabal[a], Jana Windhaber[c], Hasibullah Ehsas[a], Norbert Stockinger[a], and Johannes Boyer[a]

Objective: Measurements of pulse wave velocity are generally thought to be too impractical for clinical routine. This study aimed to develop a method that can be performed during routine 12-channel ECG.

Methods: A 12-channel ECG simultaneously supplies arterial impedance plethysmographic signals from the extremities beside segmental multifrequency impedance measurements for obtaining body composition. The origin of the plethysmographic signal (volume wave) at the arms and legs was determined at the level of the elbows and the knees. The volume wave velocity (VWV) at the aorta and femoral arteries was calculated from the time difference of the plethysmographic signals between arms and legs.

Results: Automated measurement of VWV was highly reproducible ($r = 0.96$). In 107 participants in perfect health, VWV in different models was positively related to age, physiological hemoglobin A 1C, triglycerides, normal standardized unattended blood pressure, but not to physiological low-density lipoprotein-cholesterol and high-density lipoprotein-cholesterol. Aortofemoral VWV was significantly higher in patients with established coronary artery disease than in healthy controls of the same age group (18.1 ± 5.8 vs. 11.9 ± 1.7 m/s, $P < 0.001$). VWV in study participants was higher than tonometrically determined pulse wave velocity as muscular arteries are included (13.2 ± 5.81 vs. 8.8 ± 2.98 m/s, $n = 115$, $P < 0.001$).

Conclusion: These background arterial impedance plethysmographic measurements for the measurement of VWV made simultaneously during 12-channel ECG show promise for large-scale, routine clinical assessment of large artery function.

Keywords: Combyn ECG, coronary heart disease, impedance plethysmography, pulse wave velocity

Abbreviations: (cf)PWV, (carotid-femoral) pulse wave velocity; BP, blood pressure; HbA1C, hemoglobin A1C; VWV, volume wave velocity

INTRODUCTION

Pulse wave velocity (PWV) can identify increased arterial stiffness, an additional risk factor for cardiovascular disease above and beyond traditional risk factors [1,2] especially for heart failure [3] or chronic kidney disease [4]. PWV also serves as a predictor of mortality in diabetes [5], fatal stroke [6] and coronary events [7], and hypertension [8]. Thus, PWV would seem to be an important parameter in preventive medicine, yet it has not become routine because the current procedure is cumbersome and time-consuming [9]. Attempts have been made to estimate PWV from age, blood pressure and model-based characteristic impedance [10]. Using a six-cylinder model, we previously added impedance spectroscopic and impedance plethysmographic measurements to the 12-channel ECG in order to detect an overstretched heart muscle and expanded extracellular fluid volume in chronic heart failure [11] and to measure the muscle mass of shoulders, arms, hips and legs ('appendicular muscle mass' [12]) corrected for expanded extracellular volume ('dry appendicular muscle mass') as well as body fat [13]. Nyboer *et al.* [14] had already suggested the measurement of PWV by impedance plethysmography in 1974, but without describing a possible procedure. An impedance plethysmographic method using the thoracic impedance plethysmographic signal has yielded important physiological and pathophysiological insights in the Young Finns study [15–17]. By simultaneously measuring the arterial impedance plethysmographic signals of arms and legs [11] together with the known lengths of the segments, we aimed to develop a method to study the volume wave

Journal of Hypertension 2020, 38:1989–1999

[a]Institute of Cardiovascular & Metabolic Medicine, Graz, [b]Cardiology Department, Klinikum Wels-Grieskirchen, Wels and [c]Department of Paediatric and Adolescent Surgery, Medical University Graz, Auenbruggerplatz, Graz, Austria

Correspondence to Falko Skrabal, Institute of Cardiovascular & Metabolic Medicine, Mariatrosterstr. 67, A-8043 Graz, Austria. Tel: +43 316 676767; fax: +43 316 6767674; e-mail: falko.skrabal@medunigraz.at

Received 8 November 2019 **Revised** 24 March 2020 **Accepted** 6 April 2020

DOI:10.1097/HJH.0000000000002493

velocity (VWV) of the aorta and femoral artery, its physiological determinants and to test the reproducibility of the automated measurement. The secondary objective was to compare VWV with the gold standard carotid-femoral (cf) PWV as measured by the Sphygmocor system [18]. Finally, we report a preliminary set of reference values, obtained in a sample of healthy individuals across the entire life span. We also compare results for healthy individuals with a small group of patients with established coronary heart disease (CHD) of the same age range.

MATERIALS AND METHODS

Patients

Healthy individuals and patients referred to the Institute of Cardiovascular and Metabolic Medicine in Graz, Austria, for medical checkup and training advice were invited to volunteer for this study: Biochemical risk profiles, including blood lipids and hemoglobin A 1C (HbA1C), were available only in adults. One hundred and forty-two adult participants agreed and were investigated. One hundred and seven nonsmokers were selected for perfect health; they were normotensive using repeat unobserved blood pressure measurements under standardized conditions as used in the SPRINT study [19] and had lipid levels and HbA1C within the lower normal range. To establish a provisional normal range of individuals in perfect health across the lifespan, only those 107 individuals were used as healthy controls. Also included were 405 (256 male) adolescent members of sports clubs referred to the sports outpatient unit of the Department of Paediatric and Adolescent Surgery, Medical University Graz. Furthermore, 26 patients with established CHD as indicated by past coronary intervention and/or past myocardial infarction were investigated. The study complies with the Declaration of Helsinki. It was approved by the ethics committee of the Medical University Graz (vote numbers EK 27-419 ex 14/15, 29-301 ex 16/17, 30-003 ex 17/18 and 30-466 ex 17/18) and all patients gave written informed consent.

Experimental protocol

We measured standing height to the nearest centimetre with a caliper and weight with an electronic scale to the nearest 100 g (Soehnle No. 7347).

The participants lay in a 30° head-up semi-recumbent position for at least 10 min. This position was chosen for the convenience of participants.

Blood pressure was measured automatically three times, 1 min apart in the unattended participants [19] with the Metronik BL-6 automatic blood pressure measurement device (Metronik Suess OHG, Germany).

Volume wave velocity by segmental impedance plethysmography

Using the newly developed Combyn ECG (www.ac-tc.at) [11,13], segmental impedance plethysmographic measurements were made simultaneously with the 12-channel ECG on both arms and legs. The instrument, which received CE certification in 2016, supplies alternating current of less than 50, less than 300 and less than 300 μA at 5, 40 and 400 kHz, respectively. The 40 kHz signal was used to measure the change in the impedance plethysmographic signal with the heart action to derive an arterial plethysmogram for the four extremities. Electrodes were placed as previously reported [13]: The leg and arm electrodes of the conventional ECG were replaced by double band clamp electrodes for the impedance measurements and the ECG. A double spot adhesive electrode was placed on the right side of the neck, the proximal one at the supraclavicular fossa, the distal electrode 3 cm above. The double band electrodes (4.5×1.5 cm) and the spot electrodes (diameter 2 cm) consisted of silver chloride and were moistened with ECG electrode spray. Edge-to-edge distances between current application and voltage pick-up electrodes were 3 cm. Current was applied between the two outer arm and leg electrodes. While the ECG rhythm strip was being recorded, the measurement site was switched automatically and unnoticed by the user and patient from one measurement site to the other. The arterial impedance plethysmographic signals of both arms were measured simultaneously between the inner neck and the inner arm electrodes. The leg impedance plethysmographic signals were measured simultaneously between the inner leg electrodes and the chest electrode V4, using the trunk as ionic current conductor. Using this electrode placement, the plethysmographic signal originates from the arm at the level of the elbow and from the leg at the level of the knee, respectively (see below). Templates of the signals of both arms and both legs in relation to the simultaneously recorded ECG were automatically obtained online using the arithmetic means of the peak and intersecting foot signals with the baseline. This ensured that all in all, four computer-derived time points were used to determine the time interval between the R wave of the ECG and the impedance plethysmographic signals of the arms and legs (Fig. 1). Raw signals ceased to be included when the template no longer changed by more than 1% in cross correlation. Usually, this was achieved by the inclusion of between 40 and 60 raw signals from the two arm signals and leg signals, respectively. The milliseconds between the R wave of the ECG and the intersection of the steep segment of the plethysmographic signals of arms and legs are derived automatically (Figs. 2 and 3). As can be seen, the plethysmographic arm signals are followed by the leg signals by between 50 and 100 ms. Due to the computer-assisted automatic measurements of travelling times obtained from between 40 and 60 heart beats per segment, no individuals had to be excluded for unclear measurements.

Travelling times for aortofemoral VWV were calculated in analogy to the calculation of cfPWV by subtracting the travelling times of the plethysmographic arm signals from that of the plethysmographic leg signals (Fig. 2). The measuring path (path length legs minus path length arms) was determined as follows and is explained in Fig. 2: Trunk length and leg length were measured with a measuring tape as a straight line between the suprasternal notch and the iliac band and between the iliac band and the inner ankle, respectively. A second observer ensured the verticality of the end points of trunk length measurement using a vertical ruler. As the aortic arch is located about 20% of trunk length below the suprasternal notch [20], this length was

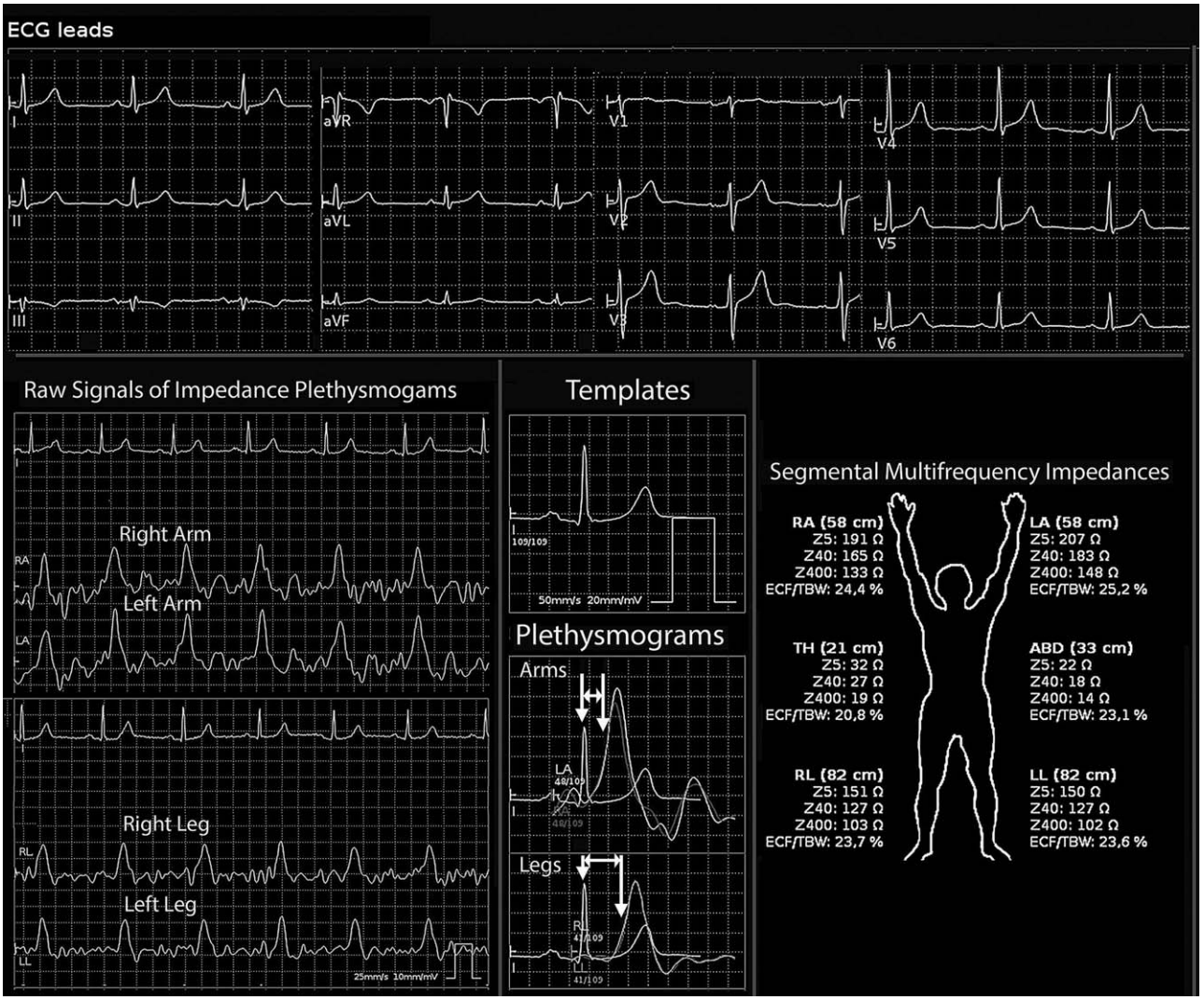

FIGURE 1 Screenshot of the output of the Combyn ECG: Top: 12 ECG leads. Bottom: Left: Raw plethysmographic signals obtained from the volume wave from both arms and legs in a representative individual. Middle: The templates of the ECG and of the plethysmographic signals are shown. Note the time delay between the R wave of the ECG and the signals from the arms and legs as indicated by the white arrows. Right: the impedances at different frequencies in the six segments from which body compartments are calculated.

subtracted from trunk length. This is also in agreement with an expert consensus document for cfPWV measurement, which recommends using 80% of the direct carotid femoral distance as travel distance for cfPWV [21]. Furthermore, as the origin of the leg plethysmogram was determined at 50% of leg length (see below), 50% of leg length was added to trunk length to obtain the travel distance of the volume wave. For the study, we also compared this path length to the body height of the patient.

Determination of the origin of the volume waves at the extremities

In order to include the whole extremities for the quantification of body composition by segmental multifrequency impedance that is also one major objective of the Combyn ECG [11], it is necessary to mount the electrodes at the wrist and ankle. This has the further advantage that the patient does not need to undress except opening the shirt for the chest electrodes. Therefore, the complete extremity is included in the measuring path and the origin of the volume wave at the extremities is uncertain. Our hypothesis was that the volume wave originated at the level of the elbow and the knee at the major reflection sites, which is the branching of the brachial and femoral arteries against which the volume wave surges. Therefore, in an additional experiment, double electrodes were mounted immediately above and below the right elbow and the left knee (Fig. 3) and arrival times were registered in 50 individuals by both methods. Arrival times of these measurements were compared with those of the conventional electrode placement.

Measurement of carotid femoral pulse wave velocity

Carotid femoral PWV was measured using a Sphygmocor device (borrowed for a limited time) in 115 patients with low and high PWV, using the intersecting tangents algorithm. For travel distance calculation, the subtracted distance (suprasternal notch-femoral site minus suprasternal notch-carotid site) was used, as this method gives best agreement with true (invasive) aortic measurements [22].

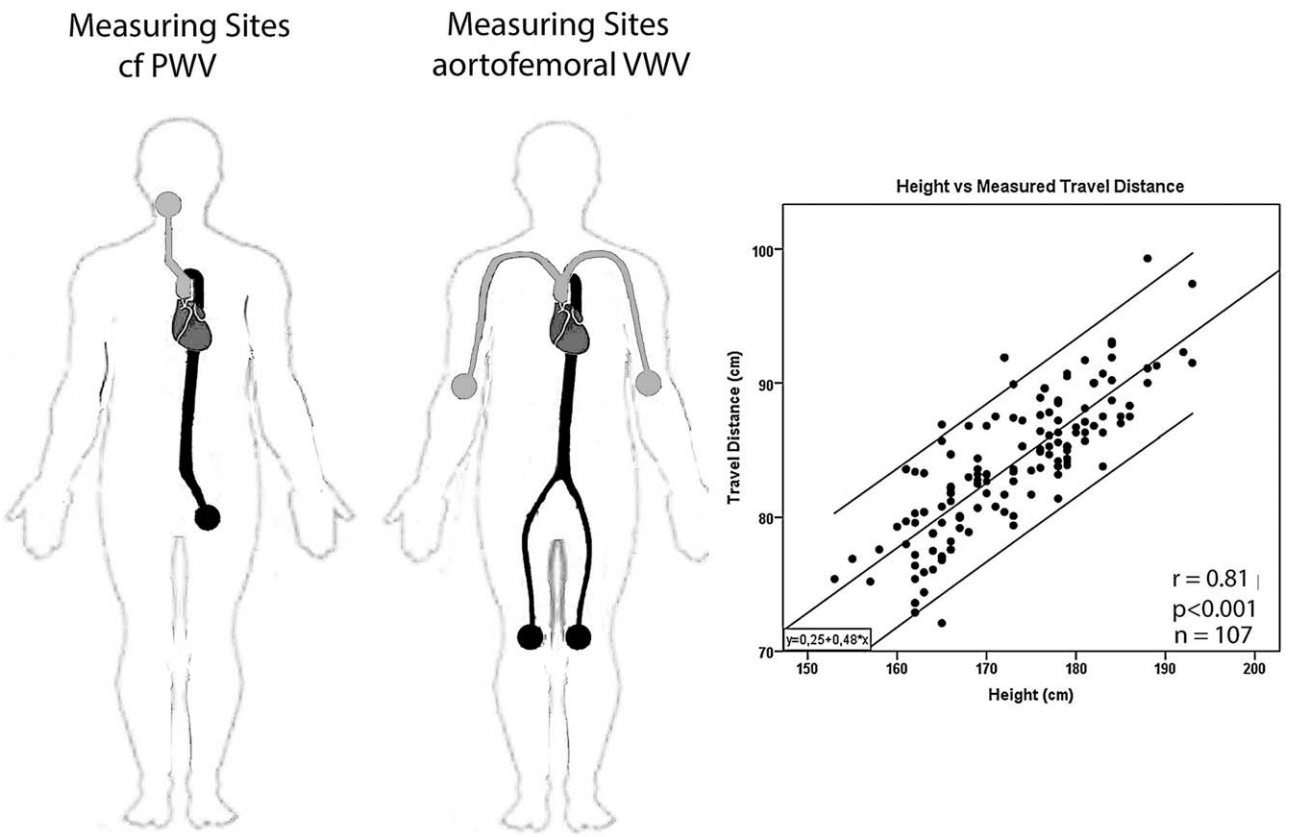

FIGURE 2 Measuring sites for carotid femoral pulse wave velocity (left) and of aortofemoral pulse wave velocity (middle). In analogy to the measurement of cfPWV, for the measurement of VWV, the time from the R wave of the ECG to the plethysmographic arm signal (shown in grey) is subtracted from the time of the R wave to the plethysmographic leg signal. This leaves the descending aorta and the femoral artery within the travelling path (shown in black). The correlation between body height and estimated travel distance is shown on the right.

Only measurements with a standard error of less than 1.5 m/s were included for further analysis. In 75 participants cfPWV and in 173 participants VWV was measured twice, 5 min apart.

Biochemical measurements

Biochemical measurements for cardiovascular risk profiling were obtained only from fasting adult participants immediately after the recording of the routine 12-channel ECG and the impedance plethysmographic signals.

These measurements included a biochemical screen, including serum creatinine, HbA1C, cholesterol, low-density lipoprotein (LDL)-cholesterol, high-density lipoprotein (HDL)-cholesterol and triglycerides. One hundred and seven participants classified as healthy during the medical checkup, which included abdominal sonography, carotid ultrasound and echocardiography, had normal values of standardized blood pressure [19] (<140/90 mmHg), glomerular filtration rate (GFR) (CKD-Epi) (>78 ml/min), cholesterol (<200 mg/dl), LDL-cholesterol (<150 mg/dl), triglycerides (<150 mg/dl) and HbA1C (<5.6%). These participants constituted the healthy control group.

Statistics

Data were analysed using the SPSS software package (version 18; SPSS Inc.,Chicago, Illinois, USA). Baseline characteristics of the study participants are given as means ± SD. Normal distribution was checked using the Kolmogorov–Smirnov test. Within the healthy control group, all parameters were normally distributed. The relationships between these variables were established using Pearson's correlation coefficients. Differences between transit times, travel distances and PWV/VWV were visualized with Bland–Altman plots. Age, sex, SBP and DBP and the measured biochemical parameters were related to VWV by multiple regression analysis using stepwise exclusion of nonsignificant parameters.

RESULTS

Baseline data including biochemical measurements of healthy participants and patients with CHD are given in Table 1.

Development of the method

Figure 3 upper shows the arrival times of the volume wave (VW) from the R wave of the ECG to the left and right arm (a) and the left and right leg (b). The plethysmographic signals of the left and right leg arrive simultaneously and are perfectly correlated (Fig. 3, upper b; 255.5 vs. 255.9 ms, mean of 107 measurements). The time difference of the arrival of the plethysmographic signals between the left and right arm was 4 ms (178.7 vs. 174.8 ms, Fig. 3, upper a), because the neck electrode was placed on the right side of the neck. This is responsible for a slightly longer measuring

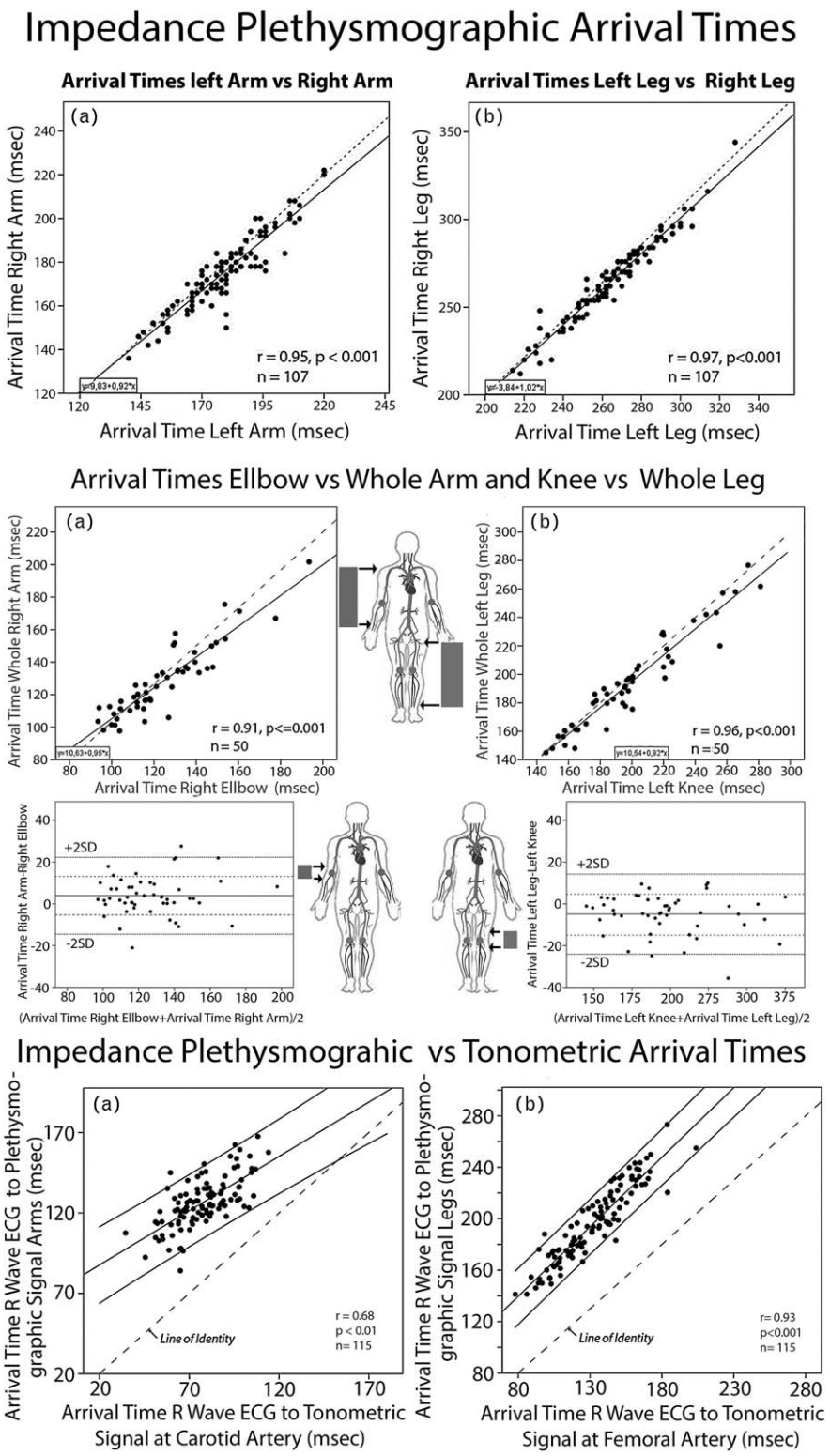

FIGURE 3 Top: Arrival times of the volume wave from the R wave of the ECG to the left and right arm artery (a) and to the left and right leg artery (b). Second: Arrival times of the volume waves at the right elbow as compared to the entire arm (a) and arrival times of the volume waves at the left knee as compared to the entire leg (b). Corresponding Bland–Altmann plots are shown below (third). Bottom: Arrival times of the volume wave vs. the tonometric signal measured from the R wave of the ECG to the carotid (a) and femoral artery (b).

path for the left arm. As blood pressure was not measured at both arms, it cannot be excluded that asymmetry of blood pressure at both arms was also responsible for the few outliers of the regression (Fig. 3, upper a).

In an attempt to clarify the origin of the plethysmographic signal (to have a rationale for travel distance measurement), we placed the electrodes immediately above and below the left knee and right elbow,

TABLE 1. Descriptive statistics for healthy individuals (left) and patients with established coronary heart disease (right)

	Healthy individuals $n = 107$		Patients with CHD $n = 26$	
	Mean	Standard deviation	Mean	Standard deviation
Age (years)	43.2	16.1	74.8	6.5
Weight (kg)	71.2	14.4	81.2	10.8
Height (cm)	172.9	8.7	173.8	8.3
BMI	23.7	3.6	26.8	3.1
SPRINT SBP* (mmHg)	117.9	13.9	138.3	19.6
SPRINT DBP (mmHg)	74.3	9.4	76.3	18.0
CKD EPI (ml/min)	95.6	17.3	71.5	17.0
Cholesterol (mg/dl)	168.9	20.4	191.2	48.9
LDL cholesterol (mg/dl)	95.2	17.8	110.4	45.5
HDL (mmol/l)	3.04	0.69	3.75	1.4
Triglycerides (mg/dl)	76.7	25.8	131.8	70.8
HBA1c (%)	5.03	0.24	5.53	0.45
VWV (m/s)	8.15	1.29	18.10	4.9

BP, blood pressure; VWV, volume wave velocity.

respectively, and compared these to the arrival times measured across the whole left leg and right arm at the y-axis (as indicated by the figurines, Fig. 3 middle). Figure 3 middle shows that the arrival times of the whole extremities and elbow/knee measurements lie on a straight line, not different from the line of identity. We conclude that the plethysmographic arm and leg signals originate at the level of the elbow and the knee. This is at the bifurcation of the brachial and femoral arteries against which the volume wave surges. Therefore, the aorta and the femoral arteries are included in the measuring path for VWV (Fig. 2).

A simplified way to estimate travel distance would be to use body height, multiplied by a correction factor. However, there was only a modest correlation between height and the measured travel distance (Fig. 2, right, $r = 0.81$, measured travel distance $= 0.48 * \text{Ht} + 0.25$, $P < 0.001$, $n = 107$).

We tested short-time reproducibility of VWV in 173 participants. The result was excellent, both measurements were almost perfectly correlated, and Bland–Altman plots supported the high reproducibility (Fig. 4, bottom). Although reproducibility of cfPWV was acceptable (Fig. 4, middle), when comparing the reproducibility of cfPWV with aortofemoral VWV, the latter was superior in this respect (Fig. 4, lower).

The arrival times of the tonometric vs. the plethysmographic signals at the upper body (Fig. 3, lowest, a) and lower body (Fig. 3, lowest, b) in 115 participants were highly correlated. According to the greater length of the measuring paths for the plethysmographic signals, the arrival times are longer than the transit time of the pulse wave from the R wave to the femoral and to carotid arteries (125 ± 16 vs. 199 ± 26 ms). For the femoral/leg signals, the correlation was shifted in parallel from the line of identity, suggesting different travel distances. The carotid pulse signals and the plethysmographic arm signals were also shifted (mean transit times 78 ± 15 vs. 134 ± 24 ms, respectively). However, in contrast to the leg signals, the slope of the regression was different from the line of identity, with differences between carotid and arm signal becoming more pronounced at shorter arrival times (i.e. higher wave speeds), suggesting that arterial segments with different mechanical properties were included.

Figure 4 upper shows the correlation and Bland–Altmann plot of cfPWV to VWV. A good correlation with low values and marked dispersion with high levels is seen. The confidence interval for mean VWV was 12.5 to 14.2 m/s, and 8.5 to 9.6 m/s for cfPWV.

Determinants of volume wave velocity, preliminary age-related reference values and comparison of healthy participants and coronary heart disease patients

As expected, VWV increases with increasing age. Figure 5 shows preliminary reference values from childhood to old age, obtained from 107 adults in perfect health (left) and 405 adolescent study participants (right). During adolescence, the rise was somewhat steeper in boys than in girls (Fig. 5, right, upper). Table 2 shows two different models of the relation of VWV to the obtained biochemistry in healthy adult participants with the exclusion of nonsignificant parameters. Age, systolic standardized BP [19], HbA1C and triglycerides within the physiological range were the determinants of VWV in the different models. Cholesterol and LDL-cholesterol within the normal range were excluded from the analysis in the different models. As a final point, VWV was faster in 26 patients with CHD older than 55 years than in 24 healthy participants also older than 55 years (18.1 ± 5.8 vs. 11.9 ± 1.66 m/s, $P < 0.001$).

DISCUSSION

Despite its potential value for risk stratification [1–7], cfPWV is currently not measured routinely in hospitals around the world for diagnostic purposes due to the cumbersome procedure; this also applies to regional PWV measurements by Doppler techniques [23], and brachial ankle PWV. The hardware and software for segmental impedance plethysmography is included in the Combyn ECG apparatus. Thus, the impedance plethysmographic method presented here has the advantage that it is measured automatically and unnoticed by staff and patients without time delay during

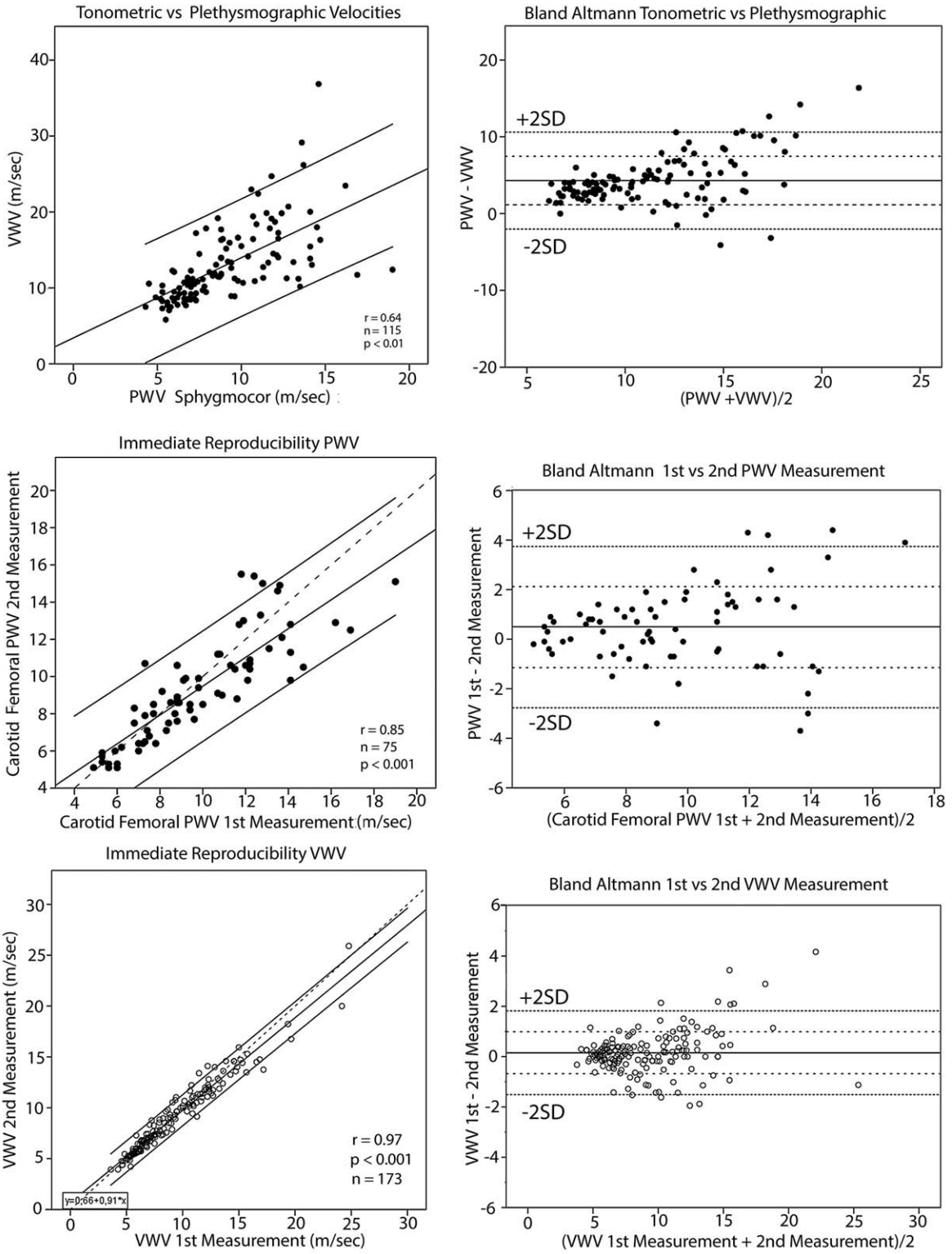

FIGURE 4 Top: Correlation of VWV and PWV measurements obtained in randomized sequence under basal conditions 5 min apart. Note the close correlation of both measures in the low range and the loose correlation with increased PWV, when stiffening of different parts of the arteries is apparent. Higher values of PWV might be due to stiffening of more central elastic parts of the measuring path. Higher values of VWV might be due to stiffening of more peripheral muscular parts of the measuring path. Middle: Reproducibility of PWV measurements, 5 min apart. Bottom: Reproducibility of VWV measurements, 5 min apart; mean blood pressures at the time of both measurements were not significantly different for both methods.

the recording of the 1 to 2-min rhythm strip of the 12-channel ECG. The results of VWV are printed out simultaneously with the printout of the 12-channel ECG. No mechanical sensors need to be placed on the body, the patient does not need to undress and sensitive areas of the body are not exposed or manipulated, which can be an

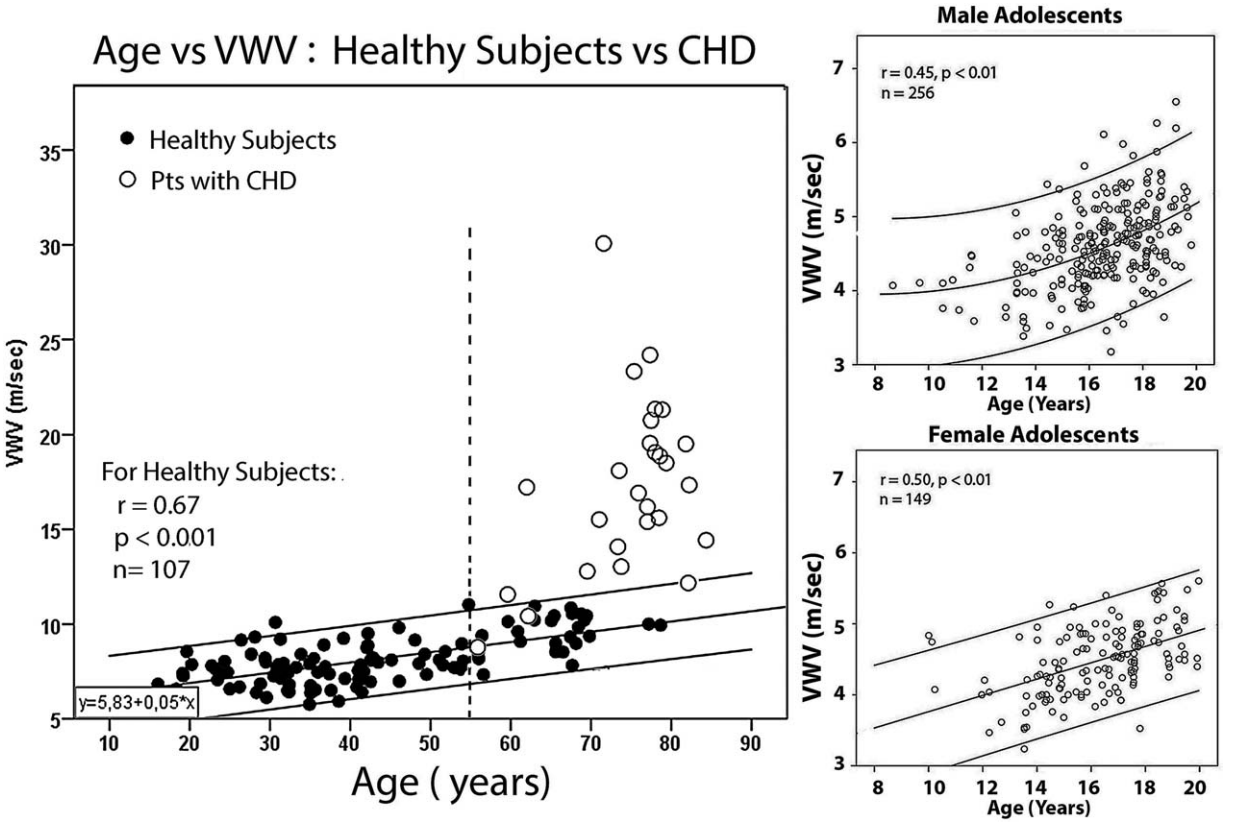

FIGURE 5 Left: Volume wave plotted against age in 107 healthy controls (black circles) and in 26 patients with established coronary heart disease (open circles). The subset of healthy controls and patients with CHD older than 55 years (right side of the dashed vertical line) showed significantly different volume wave velocities ($P < 0.001$). Right: Volume wave plotted against age in adolescent boys and girls.

advantage for individuals from diverse cultures. The patient does not notice any difference to the routine ECG apart from an additional double electrode at the neck. Thus, the methodology is very acceptable for the patients.

Here, we present the first steps in the development of this methodology. We developed technical and mathematical solutions for automated measurement. The feasibility of the method is excellent, as is the reproducibility. Major determinants of VWV (age, SBP, HbA1c) are the same as for cfPWV [24], and preliminary age-dependant reference values resemble those from the cfPWV reference value project [24]. The rise of VWV can already be observed in adolescents (Fig. 5) in whom a steeper rise in male than female adolescents occurs [25,26]. These results strongly argue for the (patho)physiological relevance of VWV.

The primary aim of our work was also to show that the determinants of VWV are those known for carotid femoral PWV. The relation of VWV to the known cardiovascular risk factors that affect cfPWV [27], namely age, SBP, HbA1C [28] argue for the physiological relevance and importance of VWV. How sensitive this new methodology is may be shown by the analysis of healthy participants: although cfPWV is known to be elevated in diabetic individuals [29–31] and triglycerides affect PWV in metabolic syndrome [32,33], we are not aware that a relation of cfPWV to HbA1C and triglycerides in healthy individuals with normal HbA1C and normal triglycerides has been shown. Here, in a stepwise backward multiple regression analysis, we demonstrate a relation of VWV to HbA1C levels in nondiabetic individuals with an HbA1C below 5.6% (Table 2). Even within the accepted lower physiological range of HbA1C below 5.6%, collagen fibres in the aorta are obviously sensitive to different levels of glycosylation [34,35]. In line with this, a correlation between HbA1C at baseline and the increase of cfPWV over 5 years has been shown in a prospective study in nondiabetic individuals [36]. This could probably be the result of an increased affinity of glycated collagen fibres for the impregnation with LDL-cholesterol [37]. In the stepwise multiple regression analysis, also normal triglycerides below 150 mg/dl are related to VWV in healthy individuals (Table 2). This could be a further argument that triglycerides represent an additional independent cardiovascular risk factor for atherosclerosis, especially CHD [38]. In contrast to HbA1C and triglycerides, in healthy individuals, normal cholesterol and LDL-cholesterol levels were not related to VWV.

A first clinical example of its usefulness is the fact that patients with established CHD had higher VWVs, when compared with healthy individuals of similar age range (18.1 ± 5.8 vs. 11.9 ± 1.66 m/s, $P < 0.001$, Fig. 5 left, age range 55–84 and 55–79 for CHD and healthy individuals, respectively). All healthy controls were normotensive at the time of the investigation. In contrast, not all patients with CHD were normotensive (Table 1) and this may partly explain the higher VWV in patients with CHD.

Determining travel distance remains an elusive goal, which is common to all different technologies: Pragmatic solutions are necessary and important, because the

TABLE 2. Multiple backward regression for volume wave velocity with exclusion of nonsignificant parameters in healthy individuals with normal unattended standardized blood pressure, normal HbA1C and normal lipids

Model 1 coefficients; dependent variable: VWV, Total $r = 0.788$					
	Not standardized coefficients		Standardized coefficients		
Model 1	B	Standard error	Beta	t	Sig.
Constant	1.045	0.909		1.150	0.253
SBP	0.050	0.008	0.396	6.083	0.000
Age	0.064	0.008	0.550	8.453	0.000

Excluded variables	Beta In	t	Sig.	Partial correlation	Collinearity statistics tolerance
BMI	0.017	0.249	0.804	0.024	0.828
HBA1C	0.016	0.233	0.816	0.023	0.762
LDL-cholesterol	−0.064	−1.058	0.293	−0.104	0.995
Triglycerides	0.106	1.712	0.090	0.166	0.927

Model 2 coefficients; dependent variable: VWV, Total $r = 0.66$					
	Not standardized coefficients		Standardized coefficients		
Model 2	B	Standard error	Beta	t	Sig.
Constant	−6.634	2.862		−2.318	0.022
HBA1C	1.537	0.602	0.200	2.553	0.012
SBP	0.063	0.010	0.504	6.434	0.000
Triglycerides	0.014	0.005	0.191	2.539	0.013

Excluded variables	Beta In	t	Sig.	Partial correlation	Collinearity statistics tolerance
HDL-cholesterol	−0.024	−0.273	0.785	−0.027	0.740
BMI	0.067	0.818	0.415	0.081	0.815
LDL-cholesterol	−0.121	−1.563	0.121	−0.153	0.894

Dependent variable: VWV.

absolute values of PWV depend critically on the determination of travel distance [39]. According to our results, there is evidence that the origin of the pulse synchronous arterial plethysmograms corresponds to the bifurcation of the brachial and femoral arteries at the level of the elbow and knee (Figs. 2 and 3) where the volume wave surges. Therefore, we calculated the travel distance as the sum of 80% of trunk length and 50% of the leg length. This is explained in Fig. 2: the aortic arch lies lower than the suprasternal notch at about 80% of trunk length and the plethysmographic leg signal arises from the bifurcation of the femoral into the anterior and posterior tibial arteries at the level of the knee, which corresponds to 50% of the leg length. Alternatively, body height multiplied by a correction factor could have been used as travel distance. As the correlation between body height and measured travel distance is modest (Fig. 2, right), we wanted to avoid losing the precision we gained by our computer assisted fully automatic measured travel times. Therefore, the measured distance and not height was used in the present analysis.

A second goal was to compare aortofemoral VWV to cfPWV: Due to the fact that the measuring path included by the cfPWV and the VWV is not identical (Fig. 2, Fig. 3 lower), we did not expect both measurements to yield the same results in the individual patient (Fig. 4 upper). The differences of the travelling times between the R wave and the plethysmograms on the one hand and the R wave and the pressure signals on the other hand also confirm that the plethysmograms arise more distally, at the middle of the arm and of the leg, and therefore, also include muscular arteries (Fig. 3 bottom). This explains the higher VWV, as the speed of propagation is faster in the latter [24,40]. The speed of the volume wave reported here on average is about the same as brachial ankle PWV [41].

The next step must be to show prospectively that VWV represents a risk factor for cardiovascular disease in addition to traditional cardiovascular risk factors, as has been shown already in the Young Finns study [17]. However, the provenance of the dZ/dt signal at the thorax is uncertain and it may originate not only from the thoracic but also from pulmonary flow [42]. Also, the B point of the impedance plethysmogram at the thorax, which is supposed to indicate the beginning of aortic flow, is variable and not located at the crossing of the base line with the upstroke of the dZ/dt signal [23,43]. This may be due to peculiar wave forms resulting, for example, from contrasting forward and backward waves [43]. In contrast, the plethysmographic arm and leg signals are exclusively the result of the contraction of the left ventricle.

The 12-channel ECG is about the only technology that is performed routinely anywhere. Impedance plethysmographic and segmental impedance measurements can be included without time delay and unnoticed by staff and patients simultaneously. In addition to diagnosing heart

failure [11], assessing hydration, appendicular muscle mass and body fat [13], these technologies performed during routine 12-channel ECG show promise for large-scale, routine clinical assessment of large artery function.

ACKNOWLEDGEMENTS

This work was supported by the Steirische Wirtschaftsförderungsgesellschaft mbH SFG, 'Geistes!Blitz' grants no. 1.000.034.146 and 1.000.037.669 and by grants no. 849750 and 855562 of the Österreichische Forschungsförderungsgesellschaft FFG, Austria. H.E., N.S. and J.B. contributed to this work during their doctoral thesis by performing preliminary studies on this topic under the supervision of F.S and of Robert Zweiker, which is gratefully acknowledged. We thank Eugenia Lamont and Ellen Zechner for language editing.

F.S. has been granted patents for the methods presented in this article. The Combyn ECG contains all the necessary hardware and software for the 12-channel ECG, segmental arterial impedance plethysmography and also segmental multifrequency impedance measurements. The instrument received CE certification in 2016, distributor: Academic Technologies (www.ac-tc.at).

This work was presented in part at the Artery 2019 conference in Budapest, Hungary.

Conflicts of interest

There are no conflicts of interest.

REFERENCES

1. Ben-Shlomo Y, Spears M, Boustred C, May M, Anderson SG, Benjamin EJ, *et al*. Aortic pulse wave velocity improves cardiovascular event prediction: an individual participant meta-analysis of prospective observational data from 17,635 subjects. *J Am Coll Cardiol* 2014; 63:636–646.
2. Mitchell GF, Hwang SJ, Vasan RS, Larson MG, Pencina MJ, Hamburg NM, *et al*. Arterial stiffness and cardiovascular events: the Framingham Heart Study. *Circulation* 2010; 121:505–511.
3. Tsao CW, Lyass A, Larson MG, Levy D, Hamburg NM, Vita JA, *et al*. Relation of central arterial stiffness to incident heart failure in the community. *J Am Heart Assoc* 2015; 4:pii: e002189.
4. Blacher J, Guerin AP, Pannier B, Marchhais SJ, Safar ME. Impact of aortic stiffness on survival in end-stage renal disease. *Circulation* 1999; 99:2434–2439.
5. Cruickshank K, Riste L, Anderson SG, Wright JS, Dunn G, Gosling RG. Aortic pulse-wave velocity and its relationship to mortality in diabetes and glucose intolerance: an integrated index of vascular function? *Circulation* 2002; 106:2085–2090.
6. Laurent S, Katsahian S, Fassot C, Tropeano AI, Gautier I, Laloux B, *et al*. Aortic stiffness is an independent predictor of fatal stroke inessential hypertension. *Stroke* 2003; 34:1203–1206.
7. Boutouyrie P, Tropeano AI, Asmar R, Gautier I, Benetos A, Lacolley P, *et al*. Aortic stiffness is an independent predictor of primary coronary events in hypertensive patients: a longitudinal study. *Hypertension* 2002; 39:10–15.
8. Laurent S, Boutouyrie P, Asmar R, Gautier I, Laloux B, Guize L, *et al*. Aortic stiffness is an independent predictor of all-cause and cardiovascular mortality in hypertensive patients. *Hypertension* 2001; 37:1236–1241.
9. Wilkinson IB, McEniery CM, Schillaci G, Boutouyrie P, Segers P, Donald A, *et al*. On behalf of the ARTERY Society. ARTERY Society guidelines for validation of non-invasive haemodynamic measurement devices: part 1, arterial pulse wave velocity. *Artery Res* 2010; 4:34–40.
10. Hametner B, Parragh S, Mayer C, Weber T, Van Bortel L, De Buyzere M, *et al*. Assessment of model based (input) impedance, pulse wave velocity, and wave reflection in the Asklepios cohort. *PLoS One* 2015; 10:e0141656.
11. Skrabal F, Pichler GP, Gratze G, Holler A. Adding "hemodynamic and fluid leads" to the ECG. Part I: the electrical estimation of BNP, chronic heart failure (CHF) and extracellular fluid (ECF) accumulation. *Med Eng Phys* 2014; 36:896–904; discussion 896.
12. Gonzalez MC, Heymsfield SB. Bioelectrical impedance analysis for diagnosing sarcopenia and cachexia: what are we really estimating? *J Cachexia Sarcopenia Muscle* 2017; 8:187–189.
13. Skrabal F, Pichler GP, Penatzer M, Steinbichl J, Hanserl AK, Leis A, *et al*. The Combyn(ECG: adding haemodynamic and fluid leads for the ECG. Part II: Prediction of total body water (TBW), extracellular fluid (ECF), ECF overload, fat mass (FM) and "dry" appendicular muscle mass (AppMM). *Med Eng Phys* 2017; 44:44–52.
14. Nyboer J, Murray P, Sedensky JA. Blood-flow indices in amputee and control limbs by mutual electrical impedance plethysmography. *Am Heart J* 1974; 87:704–710.
15. Koivistoinen T, Jula A, Aatola H, Kööbi T, Moilanen L, Lehtimäki T, *et al*. Systemic hemodynamics in relation to glucose tolerance: the Health 2000 Survey. *Metabolism* 2011; 60:557–563.
16. Koivistoinen T, Hutri-Kähönen N, Juonala M, Kööbi T, Aatola H, Lehtimäki T, *et al*. Apolipoprotein B is related to arterial pulse wave velocity in young adults: the Cardiovascular Risk in Young Finns Study. *Atherosclerosis* 2011; 214:220–224.
17. Koivistoinen T, Lyytikäinen LP, Aatola H, Luukkaala T, Juonala M, Viikari J, *et al*. Pulse wave velocity predicts the progression of blood pressure and development of hypertension in young adults. *Hypertension* 2018; 71:451–456.
18. Pannier BM, Avolio AP, Hoeks A, Mancia G, Takazawa K. Methods and devices for measuring arterial compliance in humans. *Am J Hypertens* 2002; 15:743–753.
19. The SPRINT Research Group a randomized trial of intensive versus standard blood-pressure control. *N Engl J Med* 2015; 373:2103–2116.
20. Drake RL, Vogl AW, Mitchell AWM, Tibbitts RM, Richardson PE. Gray's atlas of anatomy. 2nd ed. Edinburgh, UK: Churchill Livingstone; 2014.
21. Van Bortel LM, Laurent S, Boutouyrie P, Chowienczyk P, Cruickshank JK, De Backer T, *et al*., Artery Society; European Society of Hypertension Working Group on Vascular Structure and Function; European Network for Noninvasive Investigation of Large Arteries. Expert consensus document on the measurement of aortic stiffness in daily practice using carotid-femoral pulse wave velocity. *J Hypertens* 2012; 30:445–448.
22. Weber T, Wassertheurer S, Hametner B, Parragh S, Eber B. Noninvasive methods to assess pulse wave velocity: comparison with the invasive gold standard and relationship with organ damage. *J Hypertens* 2015; 33:1023–1031.
23. Penney BC. Theory and cardiac applications of electrical impedance measurements. *CRC Crit Rev Bioeng* 1986; 13:227–281.
24. Mattace-Raso F, Hofman A, Verwoert GC, Wittemana JC, Wilkinson I, Cockcroft J, *et al*. Determinants of pulse wave velocity in healthy people and in the presence of cardiovascular risk factors: 'establishing normal and reference values'. *Eur Heart J* 2010; 31:2338–2350.
25. Ahimastos AA, Formosa M, Dart AM, Kingwell BA. Gender differences in large artery stiffness pre- and post puberty. *J Clin Endocrinol Metab* 2003; 88:5375–5380.
26. Baguet JP, Kingwell BA, Dart AL, Shaw J, Ferrier KE, Jennings GL. Analysis of the regional pulse wave velocity by Doppler: methodology and reproducibility. *J Hum Hypertens* 2003; 17:407–412.
27. Ershova AI, Meshkov AN, Rozhkova TA, Kalinina MV, Deev AD, Rogoza AN, *et al*. Carotid and aortic stiffness in patients with heterozygous familial hypercholesterolemia. *PLoS One* 2016; 11:e0158964.
28. Teoh WL, Price JF, Williamson RM, Payne RA, Van Look LA, Reynolds RM, *et al*., ET2DS Investigators. Metabolic parameters associated with arterial stiffness in older adults with Type 2 diabetes: the Edinburgh Type 2 diabetes study. *J Hypertens* 2013; 31:1010–1017.
29. Airaksinen KE, Salmela PI, Linnaluoto MK, Ikäheimo MJ, Ahola K, Ryhänen LJ. Diminished arterial elasticity in diabetes: association with fluorescent advanced glycosylation end products in collagen. *Cardiovasc Res* 1993; 27:942–945.
30. Arnetz BB, Kallner A, Theorell T. The influence of aging on hemoglobin A1c (HbA1c). *J Gerontol* 1982; 37:648–650.
31. Scuteri A, Cunha PG, Rosei EA, Badariere J, Bekaert S, Cockcroft JR, *et al*., MARE Consortium. Arterial stiffness and influences of the metabolic syndrome: a cross-countries study. *Atherosclerosis* 2014; 233:654–660.

32. Morrison A, Hokanson JE. The independent relationship between triglycerides and coronary heart disease. *Vasc Health Risk Manag* 2009; 5:89–95.
33. Wang X, Ye P, Cao R, Yang X, Xiao W, Zhang Y, *et al*. Triglycerides are a predictive factor for arterial stiffness: a community-based 4.8-year prospective study. *Lipids Health Dis* 2016; 15:97.
34. Noh JW, Kim EJ, Seo HJ, Kim SG. Independent association between glycated hemoglobin and arterial stiffness in healthy men. *J Diabetes Investig* 2016; 7:241–246.
35. Giardino I, Edelstein D, Brownlee M. Nonenzymatic glycosylation in vitro and in bovine endothelial cells alters basic fibroblast growth factor activity. A model for intracellular glycosylation in diabetes. *J Clin Invest* 1994; 94:110–117.
36. McEniery CM, Wilkinson IB, Johansen NB, Witte DR, Singh-Manoux A, Kivimaki M, *et al*. Nondiabetic glucometabolic status and progression of aortic stiffness: the Whitehall II Study. *Diabetes Care* 2017; 40:599–606.
37. Ding C, Hsu SH, Wu YJ, Su TC. Additive effects of postchallenge hyperglycemia and low-density lipoprotein particles on the risk of arterial stiffness in healthy adults. *Lipids Health Dis* 2014; 13:179.
38. Navar AM. Editorial the evolving story of triglycerides and coronary heart disease risk. *JAMA* 2019; 321:347–349.
39. Weber T, Ammer M, Rammer M, Adji A, O'Rourke MF, Wassertheurer S, *et al*. Noninvasive determination of carotid-femoral pulse wave velocity depends critically on assessment of travel distance: a comparison with invasive measurement. *J Hypertens* 2009; 27: 1624–1630.
40. Yamashina A, Tomiyama H, Takeda K, Tsuda H, Arai T, Hirose K, *et al*. Validity, reproducibility, and clinical significance of noninvasive brachial-ankle pulse wave velocity measurement. *Hypertens Res* 2002; 25:359–366.
41. Kawasaki T, Sasayama S, Yagi S, Asakawa T, Hirai T. Non-invasive assessment of the age related changes in stiffness of major branches of the human arteries. *Cardiovasc Res* 1987; 21:678–687.
42. Malmivuo J, Plonsey R. Impedance plethysmography. In: Malmivuo J, Plonsey R, editors. *Bioelectromagnetism*. New York/Oxford: Oxford University Press; 1995. Chapter 25, pp. 540–559.
43. Ermishkin VV, Kolesnikov VA, Lukoshkova EV. Age-dependent and 'pathologic' changes in ICG waveforms resulting from superposition of pre-ejection and ejection waves. *Physiol Meas* 2014; 35:943–963.